

Gender classification via functional connectivity

GUO Siye LIU Chang WANG Zeyu ZHANG Qidan

November 20, 2024

Contents

1 Introduction

2 Materials and methods

3 Analysis

4 Discussion

Introduction

The previous work shows that there exists gender differences for structure connectivity or brain image^{[1][2][3]}:

- Women showed greater overall cortical connectivity and the underlying organization of their cortical networks was more efficient compared with men;
- Gender differences may be reflected in anatomical structures.

Some research on disease also report the gender effect^[4] or regard the gender as potential confounding effects^[5].

^[1] Gaolang Gong et al. (2009). "Age- and gender-related differences in the cortical anatomical network". en. In: *J. Neurosci.* 29, 50, pp. 15684–15693.

^[2] Mahsa Dibaji et al. (2023). "Studying the effects of sex-related differences on brain age prediction using brain MR imaging". In: *Clinical Image-Based Procedures, Fairness of AI in Medical Imaging, and Ethical and Philosophical Issues in Medical Imaging*. Cham: Springer Nature Switzerland, pp. 205–214.

^[3] Matthias Ebel et al. (2023). "Classifying sex with volume-matched brain MRI". en. In: *NeuroImage Rep.* 3, 3, p. 100181.

^[4] Mohammad S E Sendi et al. (2023). "The link between static and dynamic brain functional network connectivity and genetic risk of Alzheimer's disease". en. In: *NeuroImage Clin.* 37, 103363, p. 103363.

^[5] Weizheng Yan et al. (2019). "Discriminating schizophrenia using recurrent neural network applied on time courses of multi-site fMRI data". en. In: *EBioMedicine* 47, pp. 543–552.

Introduction

Model	Result
SVM ^[6]	across sample AUC: 0.718(± 0.2) within sample AUC: 0.716(± 0.156)
CNN ^[7]	rsfMRI AUC: 0.8923 tfMRI AUC: 0.7683
SVM ^[8]	avg ACC: 0.687 max ACC: 0.751
Partial least squares regression ^[9]	AUC: 0.93, ACC: 0.85

Table: The models and results of previous papers using static functional connectivity (sFC) to predict gender.

^[6]Obada Al Zoubi et al. (2020). "Predicting sex from resting-state fMRI across multiple independent acquired datasets".

^[7]Matthew Leming and John Suckling (2021). "Deep learning for sex classification in resting-state and task functional brain networks from the UK Biobank". en. In: *Neuroimage* 241.118409, p. 118409.

^[8]Susanne Weis et al. (2020). "Sex classification by resting state brain connectivity". en. In: *Cereb. Cortex* 30.2, pp. 824–835.

^[9]Chao Zhang et al. (2018). "Functional connectivity predicts gender: Evidence for gender differences in resting brain connectivity". en. In: *Hum. Brain Mapp.* 39.4, pp. 1765–1776.

Introduction

Model	Result
CNN and LSTM ^[10]	AUC: 0.9805, ACC: 0.9305(± 0.0191)
Statistic analysis ^[11]	Pearson dFC: ACC: 0.7984 Partial sFC: ACC: 0.9005 Pearson sFC: ACC: 0.6839
Random forest ^[12]	ACC: 0.94

Table: The models and results of previous papers using dynamic functional connectivity (dFC) to predict gender.

[10] Liangwei Fan et al. (2020). "A deep network model on dynamic functional connectivity with applications to gender classification and intelligence prediction". en. In: *Front. Neurosci.* 14, p. 881.

[11] Sreevalsan S Menon and K Krishnamurthy (2019). "A comparison of static and dynamic functional connectivities for identifying subjects and biological sex using intrinsic individual brain connectivity". en. In: *Sci. Rep.* 9.1, p. 5729.

[12] Bhaskar Sen and Keshab K Parhi (2021). "Predicting biological gender and intelligence from fMRI via dynamic functional connectivity". en. In: *IEEE Trans. Biomed. Eng.* 68.3, pp. 815–825.

HCP dataset^{[13][14]}

- Originates from brain data of more than 1000 healthy adults;
- Collects a large amount of neuroimaging data that reflects the functional connectivity of the human brain;
- Covers a variety of experimental conditions, including task state, resting state, etc;
- Widely used in various neuroscience studies, such as psychiatric studies.

^[13] Matthew F Glasser et al. (2013). "The minimal preprocessing pipelines for the Human Connectome Project". en. In: *Neuroimage* 80, pp. 105–124.

^[14] D C Van Essen et al. (2012). "The Human Connectome Project: a data acquisition perspective". en. In: *Neuroimage* 62.4, pp. 2222–2231.

Preprocessing

The following is one of the most commonly used preprocessing method^{[15][16][17][18]} (and also used by HCP dataset):

- Pre-process fMRI image data including spatial normalization, noise reduction, etc;
- Use group-ICA to decompose the brain regions;
- For each brain region, compute the representative timeseries;
- Compute the functional connectivity via partial correlation.

For the dynamic functional connectivity, we apply the sliding window method^[19] and compute the partial correlation in each window.

[15] N Filippini et al. (2009). "Distinct patterns of brain activity in young carriers of the APOE-e4 allele". In: *Proc Natl Acad Sci* 106, pp. 7209–7214.

[16] Christian F Beckmann and Stephen M Smith (2004). "Probabilistic independent component analysis for functional magnetic resonance imaging". en. In: *IEEE Trans. Med. Imaging* 23.2, pp. 137–152.

[17] Stephen M Smith et al. (2011). "Network modelling methods for fMRI". en. In: *Neuroimage* 54.2, pp. 875–891.

[18] Stephen M Smith et al. (2013). "Functional connectomics from resting-state fMRI". en. In: *Trends Cogn. Sci.* 17.12, pp. 666–682.

[19] Elena A Allen et al. (2014). "Tracking whole-brain connectivity dynamics in the resting state". en. In: *Cereb. Cortex* 24.3, pp. 663–676.

Preprocessing - Examples

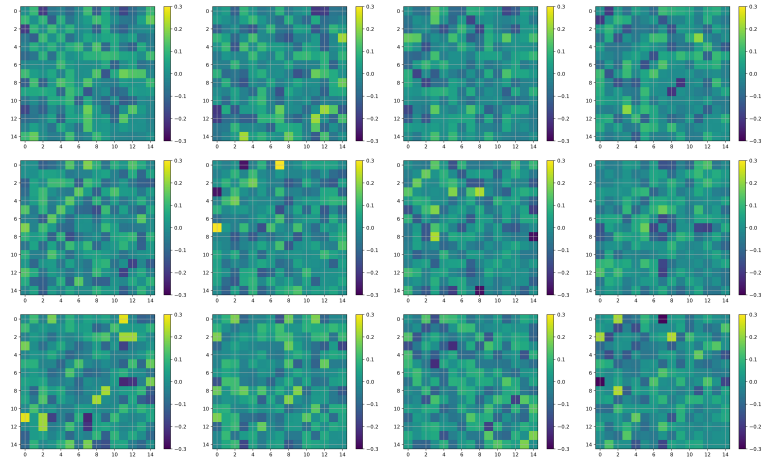


Figure: Centered dynamic functional connectivity with $N_{node} = 15$.

Preprocessing - Examples

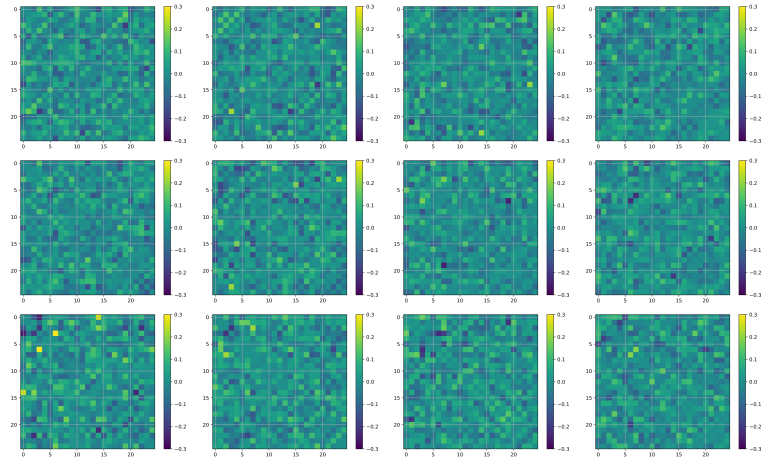


Figure: Centered dynamic functional connectivity with $N_{node} = 25$.

Preprocessing - Examples

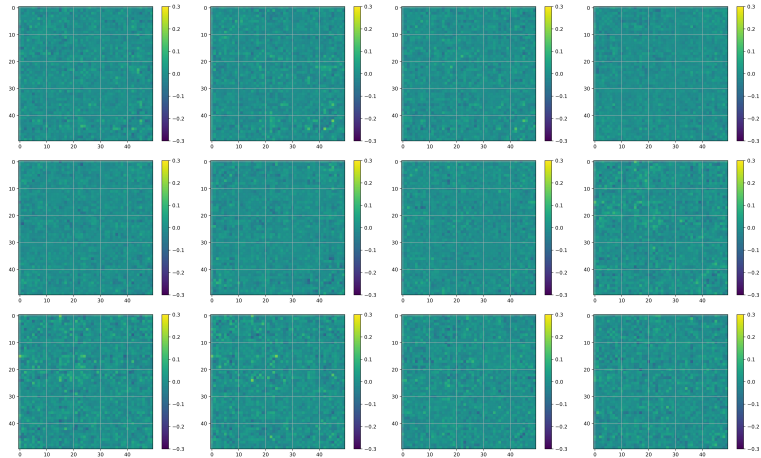


Figure: Centered dynamic functional connectivity with $N_{node} = 50$.

Preprocessing - Examples

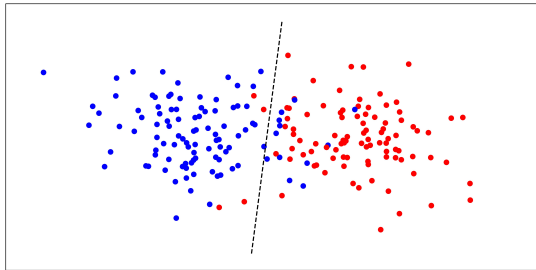
We compute the variance of each entry in dFC, which shows that the frames of dFC are more uniform with the increase of node.

N_{node}	min	mean	max
15	5.76e-6	2.80e-5	1.99e-4
25	2.82e-6	1.07e-5	6.07e-5
50	1.63e-8	1.34e-6	4.90e-6

Table: Variance of dFC

SVM^{[20][21]}

Given a dataset $\{(\mathbf{x}_i, y_i)\}_{i=1}^N$, a linear SVM aims to find a vector \mathbf{w} and a number b such that the data can be separated via the distance $\mathbf{w}^T \mathbf{x}_i - b$.



[20] Vladimir N Vapnik (1997). "The support vector method". In: *Lecture Notes in Computer Science*. Berlin, Heidelberg: Springer Berlin Heidelberg, pp. 261–271.

[21] Corinna Cortes and Vladimir Vapnik (1995). "Support-vector networks". en. In: *Mach. Learn.* 20.3, pp. 273–297.

SVM - Results

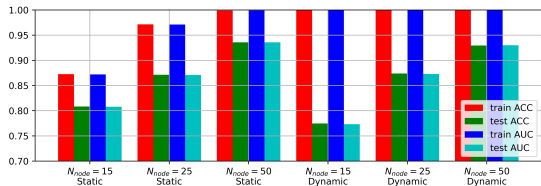


Figure: Results of Linear SVM.

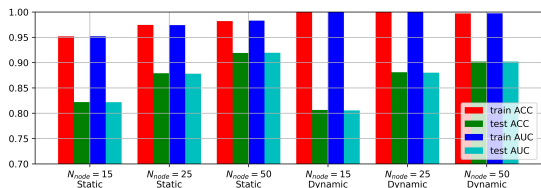
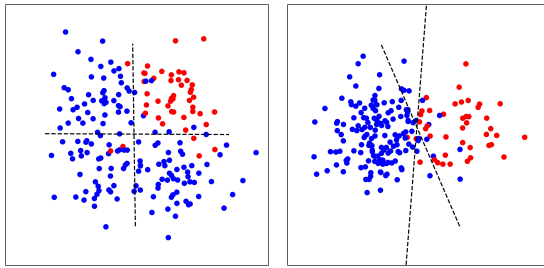


Figure: Results of Nu-SVM.

CNN - Model

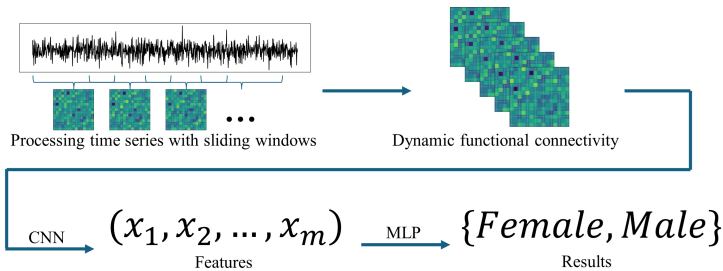
Given a dataset $\{(\mathbf{x}_i, y_i)\}_{i=1}^N$, we aim to find some vectors $\{\mathbf{w}_k\}_{k=1}^m$ and some numbers $\{b_k\}_{k=1}^m$ such that any given data \mathbf{x} can be classified via the tuple of distance $(\mathbf{w}_1^T \mathbf{x} - b_1, \dots, \mathbf{w}_m^T \mathbf{x} - b_m)$.

In the worst case, all the \mathbf{w}_k and b_k are the same, then the results should be the same with linear SVM.



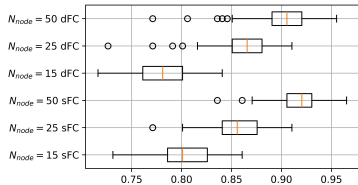
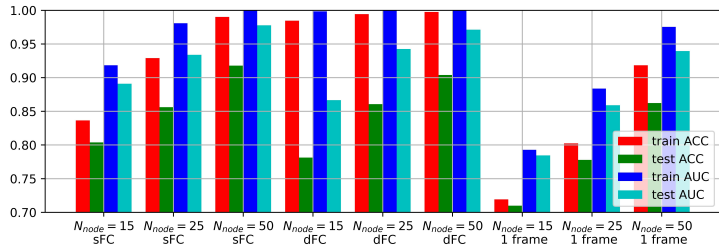
CNN - Model

The followings are the flowchart of our method, where we use a 1-layer 1-dimensional CNN with size equivalent to the input shape, so that it is the same as previous statements.

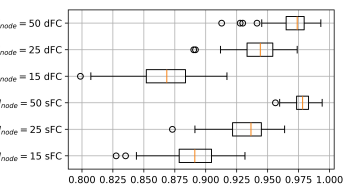


We split the data into training dataset (80%) and test dataset (20%), and repeat the experiment for 150 times to avoid flukes.

CNN - Results



(a) test ACC



(b) test AUC

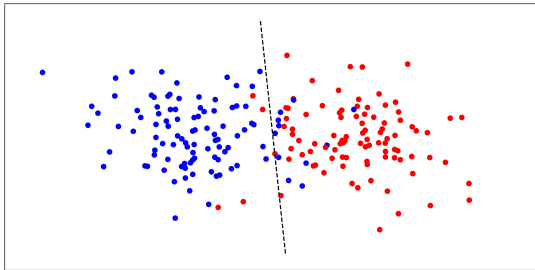
Figure: Results of CNN model with dropout = 0.1 and channel = 4.

CNN - Results

- More nodes leads to a higher accuracy and AUC;
- The choice of sFC and dFC will not significantly affect the result;
- The accuracy rate will decrease when using the sub-series.

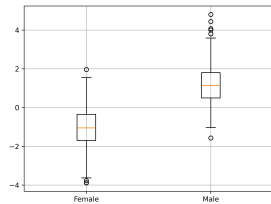
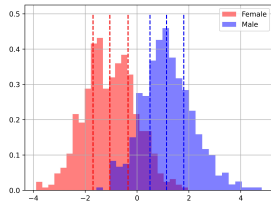
LDA^[22]

Given a dataset $\{\mathbf{x}_i, y_i\}_{i=1}^N$, the LDA aims to find a vector pair \mathbf{y}, \mathbf{c} such that the inner product $\langle \mathbf{x}_i - \mathbf{c}, \mathbf{y} \rangle$ minimizes the interclass variance and maximizes the distance between the projected means of the classes.

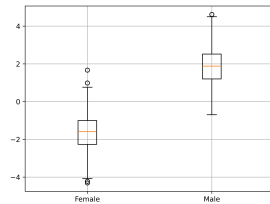
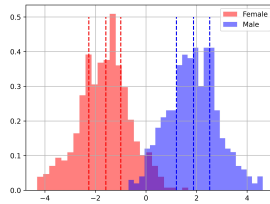


^[22]Harvey Goldstein, Jacob Cohen, and Patricia Cohen (1976). "Applied multiple regression/correlation analysis for the behavioural sciences". In: *J. R. Stat. Soc. Ser. A* 139.4, p. 549.

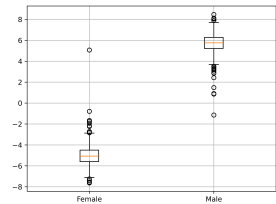
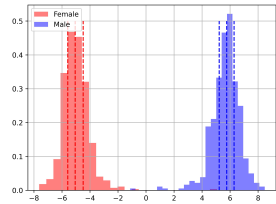
LDA - sFC



(a) $N_{node} = 15$



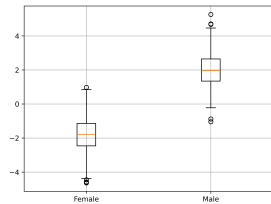
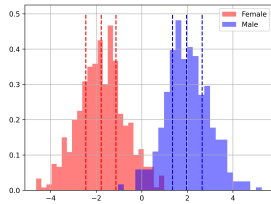
(b) $N_{node} = 25$



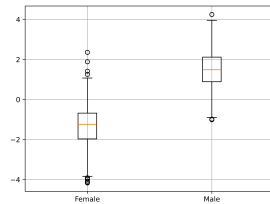
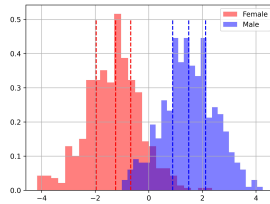
(c) $N_{node} = 50$

Figure: LDA for sFC.

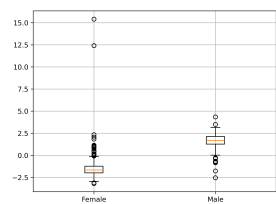
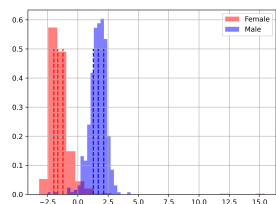
LDA - dFC



(a) $N_{node} = 15$



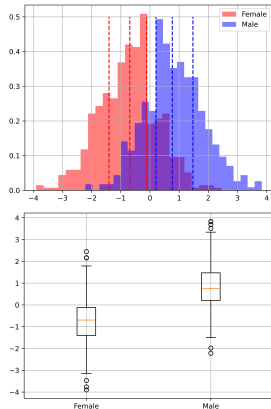
(b) $N_{node} = 25$



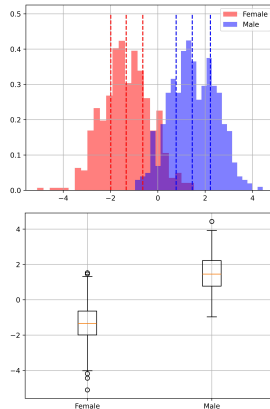
(c) $N_{node} = 50$

Figure: LDA for dFC.

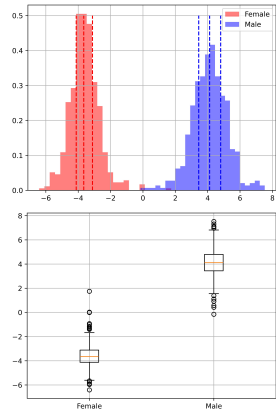
LDA - dFC



(a) $N_{node} = 15$



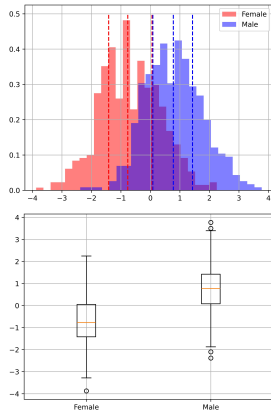
(b) $N_{node} = 25$



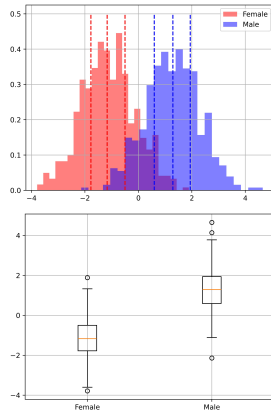
(c) $N_{node} = 50$

Figure: LDA for 1-frame of dFC with max score.

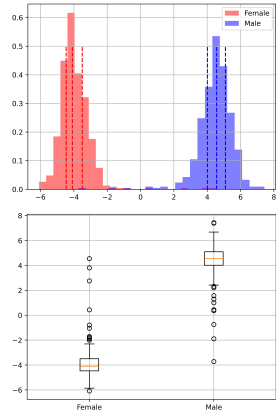
LDA - dFC



(a) $N_{node} = 15$



(b) $N_{node} = 25$



(c) $N_{node} = 50$

Figure: LDA for 1-frame of dFC with min score.

LDA - Results

- Both sFC and dFC is linear separable;
- The overlap become less with the increase of node;
- The dFC is not always better than sFC, especially when there exists some outliers.

Discussion

- Both sFC and dFC is linear separable;
- Both sFC and dFC can be used to predict gender with high accuracy and AUC;
- More nodes leads to a higher accuracy and AUC;
- The choice of sFC and dFC will not significantly affect the accuracy rate and AUC;
- The brain noise^[23] will affect more on the dFC.

^[23]spontaneous fluctuations in the electrical activity of the neurons

Future research directions

- Choose a more reasonable size and step of the window via Fourier analysis, wavelet analysis, etc;
- Force the coefficient of CNN to be orthogonal;
- Use some simple nonlinear classifier (i.e. quadratic classifier);
- Use effective connectivity as input.

Reference I

-  Al Zoubi, Obada et al. (2020). "Predicting sex from resting-state fMRI across multiple independent acquired datasets".
-  Allen, Elena A et al. (2014). "Tracking whole-brain connectivity dynamics in the resting state". en. In: *Cereb. Cortex* 24.3, pp. 663–676.
-  Beckmann, Christian F and Stephen M Smith (2004). "Probabilistic independent component analysis for functional magnetic resonance imaging". en. In: *IEEE Trans. Med. Imaging* 23.2, pp. 137–152.
-  Cortes, Corinna and Vladimir Vapnik (1995). "Support-vector networks". en. In: *Mach. Learn.* 20.3, pp. 273–297.
-  Dibaji, Mahsa et al. (2023). "Studying the effects of sex-related differences on brain age prediction using brain MR imaging". In: *Clinical Image-Based Procedures, Fairness of AI in Medical Imaging, and Ethical and Philosophical Issues in Medical Imaging*. Cham: Springer Nature Switzerland, pp. 205–214.

Reference II

-  Ebel, Matthis et al. (2023). "Classifying sex with volume-matched brain MRI". en. In: *Neuroimage Rep.* 3.3, p. 100181.
-  Fan, Liangwei et al. (2020). "A deep network model on dynamic functional connectivity with applications to gender classification and intelligence prediction". en. In: *Front. Neurosci.* 14, p. 881.
-  Filippini, N et al. (2009). "Distinct patterns of brain activity in young carriers of the APOE-e4 allele". In: *Proc Natl Acad Sci* 106, pp. 7209–7214.
-  Glasser, Matthew F et al. (2013). "The minimal preprocessing pipelines for the Human Connectome Project". en. In: *Neuroimage* 80, pp. 105–124.
-  Goldstein, Harvey, Jacob Cohen, and Patricia Cohen (1976). "Applied multiple regression/correlation analysis for the behavioural sciences". In: *J. R. Stat. Soc. Ser. A* 139.4, p. 549.

Reference III

-  Gong, Gaolang et al. (2009). "Age- and gender-related differences in the cortical anatomical network". en. In: *J. Neurosci.* 29.50, pp. 15684–15693.
-  Leming, Matthew and John Suckling (2021). "Deep learning for sex classification in resting-state and task functional brain networks from the UK Biobank". en. In: *Neuroimage* 241.118409, p. 118409.
-  Menon, Sreevalsan S and K Krishnamurthy (2019). "A comparison of static and dynamic functional connectivities for identifying subjects and biological sex using intrinsic individual brain connectivity". en. In: *Sci. Rep.* 9.1, p. 5729.
-  Sen, Bhaskar and Keshab K Parhi (2021). "Predicting biological gender and intelligence from fMRI via dynamic functional connectivity". en. In: *IEEE Trans. Biomed. Eng.* 68.3, pp. 815–825.

Reference IV

-  Sendi, Mohammad S E et al. (2023). "The link between static and dynamic brain functional network connectivity and genetic risk of Alzheimer's disease". en. In: *NeuroImage Clin.* 37.103363, p. 103363.
-  Smith, Stephen M et al. (2011). "Network modelling methods for fMRI". en. In: *Neuroimage* 54.2, pp. 875–891.
-  Smith, Stephen M et al. (2013). "Functional connectomics from resting-state fMRI". en. In: *Trends Cogn. Sci.* 17.12, pp. 666–682.
-  Van Essen, D C et al. (2012). "The Human Connectome Project: a data acquisition perspective". en. In: *Neuroimage* 62.4, pp. 2222–2231.
-  Vapnik, Vladimir N (1997). "The support vector method". In: *Lecture Notes in Computer Science*. Berlin, Heidelberg: Springer Berlin Heidelberg, pp. 261–271.
-  Weis, Susanne et al. (2020). "Sex classification by resting state brain connectivity". en. In: *Cereb. Cortex* 30.2, pp. 824–835.

Reference V

-  Yan, Weizheng et al. (2019). "Discriminating schizophrenia using recurrent neural network applied on time courses of multi-site fMRI data". en. In: *EBioMedicine* 47, pp. 543–552.
-  Zhang, Chao et al. (2018). "Functional connectivity predicts gender: Evidence for gender differences in resting brain connectivity". en. In: *Hum. Brain Mapp.* 39.4, pp. 1765–1776.

Ablation study - SVM

Node	Data	min ACC/AUC	mean ACC/AUC	max ACC/AUC
15	sFC	0.7363/0.7369	0.8083/0.8078	0.8706/0.8756
25	sFC	0.8060/0.8059	0.8714/0.8708	0.9204/0.9202
50	sFC	0.8905/0.8905	0.9357/0.9357	0.9751/0.9749
15	dFC	0.6866/0.6919	0.7746/0.7733	0.8507/0.8534
25	dFC	0.7861/0.7874	0.8739/0.8730	0.9204/0.9206
50	dFC	0.8806/0.8813	0.9295/0.9300	0.9652/0.9666

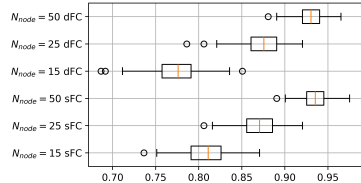
Table: Ablation study for LinearSVM.

Ablation study - SVM

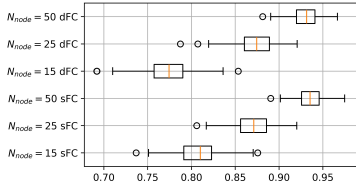
Node	Data	min ACC/AUC	mean ACC/AUC	max ACC/AUC
15	sFC	0.7562/0.7571	0.8221/0.8219	0.8856/0.8847
25	sFC	0.8259/0.8257	0.8791/0.8782	0.9303/0.9302
50	sFC	0.8458/0.8458	0.9191/0.9194	0.9602/0.9608
15	dFC	0.7313/0.7324	0.8066/0.8056	0.8706/0.8674
25	dFC	0.8109/0.8121	0.8811/0.8802	0.9303/0.9296
50	dFC	0.8308/0.8300	0.9021/0.9022	0.9552/0.9579

Table: Ablation study for NuSVM.

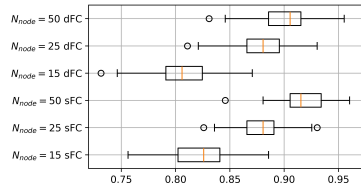
Ablation study - SVM



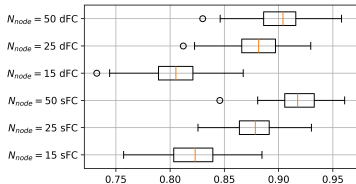
(a) test ACC for LinearSVM



(b) test AUC for LinearSVM



(c) test ACC for NuSVM



(d) test AUC for NuSVM

Figure: Results of SVM.

Ablation study - CNN

Data	DR	CH	min ACC/AUC	mean ACC/AUC	max ACC/AUC
sFC	0.0	1	0.5224/0.8108	0.7957/0.8855	0.8706/0.9307
sFC	0.0	2	0.7164/0.8273	0.8001/0.8876	0.8756/0.9281
sFC	0.0	4	0.7363/0.8189	0.7988/0.8863	0.8607/0.9337
sFC	0.1	1	0.5174/0.8041	0.7952/0.8870	0.8756/0.9355
sFC	0.1	2	0.7164/0.8318	0.7986/0.8885	0.8756/0.9294
sFC	0.1	4	0.7313/0.8276	0.8038/0.8911	0.8607/0.9317
dFC	0.0	1	0.5871/0.7160	0.7737/0.8670	0.8557/0.9216
dFC	0.0	2	0.6915/0.7824	0.7811/0.8630	0.8507/0.9209
dFC	0.0	4	0.7015/0.8028	0.7787/0.8584	0.8408/0.9148
dFC	0.1	1	0.5522/0.7140	0.7735/0.8656	0.8458/0.9209
dFC	0.1	2	0.6617/0.7942	0.7771/0.8692	0.8408/0.9110
dFC	0.1	4	0.7164/0.7987	0.7813/0.8666	0.8408/0.9171

Table: Ablation study for $N_{node} = 15$.

Ablation study - CNN

Data	DR	CH	min ACC/AUC	mean ACC/AUC	max ACC/AUC
sFC	0.0	1	0.5075/0.7475	0.8462/0.9265	0.9104/0.9634
sFC	0.0	2	0.7662/0.8731	0.8470/0.9225	0.9104/0.9599
sFC	0.0	4	0.7512/0.8650	0.8468/0.9220	0.9055/0.9603
sFC	0.1	1	0.5124/0.7431	0.8547/0.9356	0.9154/0.9688
sFC	0.1	2	0.7711/0.8598	0.8581/0.9358	0.9254/0.9728
sFC	0.1	4	0.7711/0.8730	0.8562/0.9339	0.9104/0.9638
dFC	0.0	1	0.6269/0.7168	0.8450/0.9338	0.9303/0.9788
dFC	0.0	2	0.7463/0.8662	0.8594/0.9416	0.9254/0.9787
dFC	0.0	4	0.7960/0.9130	0.8672/0.9437	0.9154/0.9783
dFC	0.1	1	0.5771/0.6996	0.8391/0.9319	0.9254/0.9753
dFC	0.1	2	0.7612/0.8584	0.8618/0.9441	0.9204/0.9752
dFC	0.1	4	0.7264/0.8902	0.8606/0.9426	0.9104/0.9739

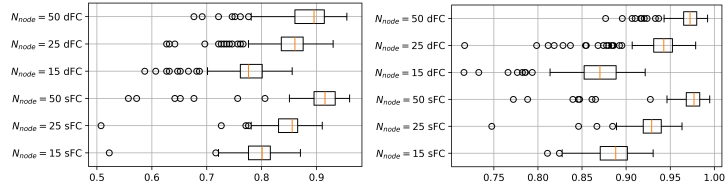
Table: Ablation study for $N_{node} = 25$.

Ablation study - CNN

Data	DR	CH	min ACC/AUC	mean ACC/AUC	max ACC/AUC
sFC	0.0	1	0.5572/0.7721	0.9015/0.9689	0.9602/0.9947
sFC	0.0	2	0.7512/0.8462	0.9218/0.9762	0.9701/0.9941
sFC	0.0	4	0.8856/0.9589	0.9248/0.9779	0.9602/0.9938
sFC	0.1	1	0.5124/0.7691	0.8960/0.9684	0.9652/0.9952
sFC	0.1	2	0.7363/0.8335	0.9147/0.9746	0.9652/0.9947
sFC	0.1	4	0.8358/0.9562	0.9178/0.9778	0.9652/0.9940
dFC	0.0	1	0.6766/0.8767	0.8799/0.9689	0.9552/0.9924
dFC	0.0	2	0.7711/0.9366	0.9041/0.9733	0.9552/0.9917
dFC	0.0	4	0.8507/0.9543	0.9122/0.9766	0.9602/0.9946
dFC	0.1	1	0.7363/0.8511	0.8945/0.9714	0.9602/0.9940
dFC	0.1	2	0.8109/0.8966	0.9027/0.9716	0.9552/0.9925
dFC	0.1	4	0.7711/0.9128	0.9040/0.9713	0.9552/0.9930

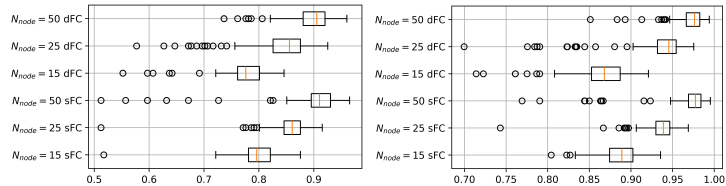
Table: Ablation study for $N_{node} = 50$.

Ablation study - CNN



(a) test ACC with dropout=0.0

(b) test AUC with dropout=0.0

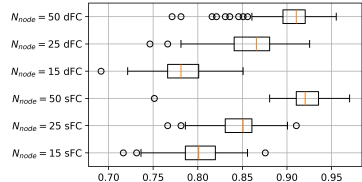


(c) test ACC with dropout=0.1

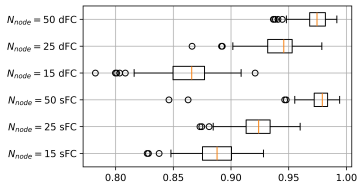
(d) test AUC with dropout=0.1

Figure: Results of CNN model with channel = 1.

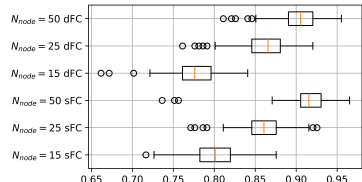
Ablation study - CNN



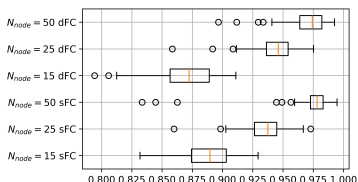
(a) test ACC with dropout=0.0



(b) test AUC with dropout=0.0



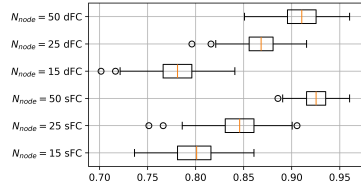
(c) test ACC with dropout=0.1



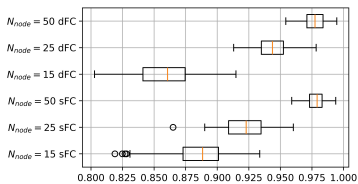
(d) test AUC with dropout=0.1

Figure: Results of CNN model with channel = 2.

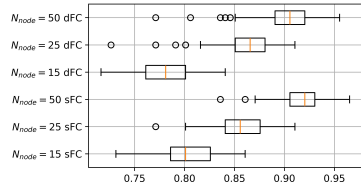
Ablation study - CNN



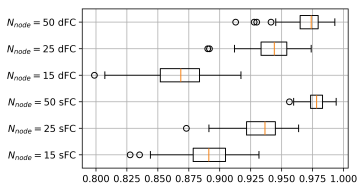
(a) test ACC with dropout=0.0



(b) test AUC with dropout=0.0



(c) test ACC with dropout=0.1



(d) test AUC with dropout=0.1

Figure: Results of CNN model with channel = 4.

Ablation study - Repeat time

Assume that the results (AUC or ACC) $\{X_i\}_{i=1}^n$ for different test are iid with mean value μ and variance σ^2 , then from central limit theorem

$$Y_n = \frac{\sum_{i=1}^n X_i - n\mu}{\sqrt{n}\sigma} \xrightarrow{D} N(0, 1).$$

Thus for all $\varepsilon > 0$,

$$P\left(\left|\bar{X}_i - \mu\right| \leq \frac{\sigma\varepsilon}{\sqrt{n}}\right) = P(|Y_n - E(Y_n)| \leq \varepsilon) = \Phi(\varepsilon) - \Phi(-\varepsilon),$$

where $\Phi(x)$ is the cumulative distribution function of the standard normal distribution.

Ablation study - Repeat time

We compute the variance of samples $\sigma \leq \sqrt{0.007} \leq 0.1$, which implies that if choose $\varepsilon = \sqrt{n}/\delta$, then

$$P\left(|(\bar{X}_i - \mu)| \leq \frac{0.1}{\delta}\right) \geq P\left(|\bar{X}_i - \mu| \leq \frac{\sigma}{\delta}\right) = \Phi\left(\frac{\sqrt{n}}{\delta}\right) - \Phi\left(-\frac{\sqrt{n}}{\delta}\right).$$

For $n = 150$,

- When choose $\delta = 5$, $P(|\bar{X}_i - \mu| \leq 0.02) \geq 0.9857$;
- When choose $\delta = 8$, $P(|\bar{X}_i - \mu| \leq 0.0125) \geq 0.8742$;
- When choose $\delta = 10$, $P(|\bar{X}_i - \mu| \leq 0.01) \geq 0.7793$;
- When choose $\delta = 12.5$, $P(|\bar{X}_i - \mu| \leq 0.008) \geq 0.6728$;
- When choose $\delta = 16$, $P(|\bar{X}_i - \mu| \leq 0.00625) \geq 0.5560$;
- When choose $\delta = 20$, $P(|\bar{X}_i - \mu| \leq 0.005) \geq 0.4597$.